Biomedicine & Pharmacotherapy 165 (2023) 115055

Contents lists available at ScienceDirect

Biomedicine & Pharmacotherapy

journal homepage: www.elsevier.com/locate/biopha

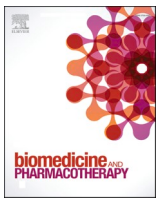

Morphine-withdrawal aversive memories and their extinction modulate H4K5 acetylation and Brd4 activation in the rat hippocampus and basolateral amygdala

Aurelio Franco-García [a,b], Victoria Gómez-Murcia [a,b], Francisco José Fernández-Gómez [a,b], Raúl González-Andreu [a], Juana M. Hidalgo [a,b], M. Victoria Milanés [a,b,*], Cristina Núñez [a,b,*]

[a] Group of Cellular and Molecular Pharmacology, Department of Pharmacology, CEIR Campus Mare Nostrum, University of Murcia, Spain
[b] Instituto Murciano de Investigación Biosanitaria (IMIB) – Pascual Parrilla, Murcia, Spain

ARTICLE INFO

Keywords:
Opioid aversive memories
Extinction
Epigenetic marks
Brd4
Basolateral amygdala
Hippocampus

ABSTRACT

Chromatin modification is a crucial mechanism in several important phenomena in the brain, including drug addiction. Persistence of drug craving and risk of relapse could be attributed to drug-induced epigenetic mechanisms that seem to be candidates explaining long-lasting drug-induced behaviour and molecular alterations. Histone acetylation has been proposed to regulate drug-seeking behaviours and the extinction of rewarding memory of drug taking. In this work, we studied the epigenetic regulation during conditioned place aversion and after extinction of aversive memory of opiate withdrawal. Through immunofluorescence assays, we assessed some epigenetic marks (H4K5ac and p-Brd4) in crucial areas related to memory retrieval -basolateral amygdala (BLA) and hippocampus-. Additionally, to test the degree of transcriptional activation, we evaluated the immediate early genes (IEGs) response (*Arc, Bdnf, Creb, Egr-1*, *Fos* and *Nfkb*) and *Smarcc1* (chromatin remodeler) through RT-qPCR in these nuclei. Our results showed increased p-Brd4 and H4K5ac levels during aversive memory retrieval, suggesting a more open chromatin state. However, transcriptional activation of these IEGs was not found, therefore suggesting that other secondary response may already be happening. Additionally, *Smarcc1* levels were reduced due to morphine chronic administration in BLA and dentate gyrus. The activation markers returned to control levels after the retrieval of aversive memories, revealing a more repressed chromatin state. Taken together, our results show a major role of the tandem H4K5ac/p-Brd4 during the retrieval of aversive memories. These results might be useful to elucidate new molecular targets to improve and develop pharmacological treatments to address addiction and to avoid drug relapse.

1. Introduction

Drug addiction, including opiate addiction, is a chronically relapsing disorder characterized by compulsive drug seeking and use. A central problem in opiate addiction treatment is high rates of relapse to opiate use during abstinence [1,2]. One of the factors thought to be responsible for that vulnerability is conditioned withdrawal, which consists in somatic and/or affective signs elicited in presence of cues that were previously paired with drug withdrawal [3]. Conditioned-place aversion (CPA) is a highly sensitive associative learning animal model for measurement of the negative affective components of opiate withdrawal [4–6]. CPA paradigm involves both memory formation, in which the environment acquires negative emotional salience, and also memory retrieval, where the aversive affective memory can be reactivated and evoked by contextual cues [7]. Reactivation of this aversive affective memories requires synaptic plasticity and has been suggested to trigger the relapse of drug-seeking behaviour in abstinent addicts [5, 8–12]. The updating or editing process of emotional valent drug-related memories

Abbreviations: BLA, basolateral amygdala; CPA, conditioned place aversion; CPP, conditioned place preference; DG, dentate gyrus; HAT, histone acetyltransferase; H4K5ac, acetylation of lysine 5 of histone H4; IEGs, immediate early genes; IR, immunoreactivity; MAP, Maximum intensity projection; M1, Manders' overlap coefficient 1; M2, Manders' overlap coefficient 2; NAc, nucleus accumbens; PCC, Pearson's correlation coefficient; VTA, ventral tegmental area.

* Correspondence to: Department of Pharmacology, Universidad de Murcia, Murcia, Spain; Biomedical Research Institute of Murcia (IMIB-Arrixaca), Carretera de Buenavista, 30120 Murcia, Spain

E-mail addresses: milanes@um.es (M. Victoria Milanés), crisnp@um.es (C. Núñez).

https://doi.org/10.1016/j.biopha.2023.115055
Received 30 March 2023; Received in revised form 13 June 2023; Accepted 21 June 2023

has shown to modify behavioural outcomes, hence preventing the retrieval of drug-associated memories [13]. In this line of evidence, extinction therapy has been proposed as a method to reduce the motivational impact of drug-associated cues to prevent relapse [14–16]. Improved understanding of the circuit mechanisms mediating both extinction and cue-induced relapse to opiate seeking is critical for the development of effective behavioural and pharmacological treatment of opiate addiction [17].

Chromatin modification is increasingly recognized as a crucial mechanism in several important phenomena in the brain, including drug addiction. Growing evidence during the last years has suggested that the persistence of drugs craving and risk of relapse could be attributed to drug-induced epigenetic mechanisms that seem to be candidates explaining long-lasting drug-induced molecular alterations [18,19]. Modifications of histone acetylation have been found to regulate drug-seeking behaviours and the extinction of rewarding memory of drug taking [20,21].

Recent evidence suggests that regulation of histone acetylation via histone acetyltransferases (HATs) is attractive candidate in reward-related brain regions for regulation of memory formation of addiction to psychostimulants like cocaine [22,23], whereas research into opiate-induced changes to the epigenetic landscape is beginning to emerge. Since epigenetic changes during drug abstinence and/or extinction training could be very important for further relapse prevention therapy, the present experiments were designed to study epigenetic regulation during CPA and after extinction of aversive memory of opiate withdrawal. This study examined whether aversive memory of morphine withdrawal and/or the neutral memory after the extinction training are concurrent with chromatin remodelling. To accomplish this, in our study we performed the analysis of acetylation changes of lysine 5 on histone H4 (H4K5ac) and other mechanisms involved in chromatin remodelling, such as Brd4, during the retrieval of morphine-withdrawal (abstinence) memory as well as after extinction training procedure by using a CPA paradigm in rats. On the other hand, Smarcc1 protein has shown to play a major role in transcriptional activity as a molecular switch controlling mRNA synthesis [24]. Since H4K5/8/12/16Ac has been shown to be markers of transcriptional activation induced by drugs of abuse [25], and *Smarcc1* has been proposed to be crucial for chromatin remodelling [26], the influence of CPA and extinction training on the transcript of *Smarcc1* was determined. Further, we have studied whether the observed epigenetic changes in the present work are paralleled with modification of expression of genes identified as relevant in the context of neuronal activity and neuroplasticity.

We focused our study on in different memory-related brain regions such as hippocampus (dentate gyrus -DG, CA1 and CA3) and basolateral amygdaloid nucleus (BLA), since BLA represents a critical neural substrate among the limbic areas that are likely to mediate motivational features of opiate dependence, [27,28] and is part of an integrated circuit of neuronal structures implicated in the formation and storage of conditioned stimulus [(specific environmental context-unconditioned stimulus (naloxone-precipitated morphine withdrawal)] associations and in the processing of emotional events in relation to environmental stimuli that guide motivated behaviour [29]. On the other hand, the hippocampus is crucially important not only for memory encoding/consolidation but also for episodic memory retrieval [30].

2. Methods

2.1. Animals

Wistar male adult rats (220–240 g at the beginning of the experiment) were housed in methacrylate cages (length: 45 cm; width: 24 cm; height: 20 cm; 2–3 rats per cage) under a 12 h light/dark cycle (light: 8:00–20:00 h) in a room with controlled temperature (22 ± 2 °C). Food and water were available ad libitum. Animals were conditioned and tested during the light phase of the cycle. They were handled daily during the first week after arrival to minimise stress. All surgical and experimental procedures were performed in accordance with the European Communities Council Directive of 22 September 2010 (2010/63/UE) and were approved by the local Committees for animal research (Comité de Ética y Experimentación Animal; CEEA; RD 53/2013; REGA ES300305440012).

2.2. Drugs

Morphine base was obtained from Alcaliber Laboratories (Madrid, Spain). Morphine was administered as pellets of sustained release containing morphine base (75 mg), Avicel (55 mg), polyvinylpyrrolidone (20 mg), Aerosil (0.75 mg) and magnesium stearate (1.5 mg). Placebo pellets contained the same compounds, but morphine base was replaced with lactose. Naloxone hydrochloride was purchased from Sigma Chemical (St. Louis, MO, USA), dissolved in sterile saline (0.9% NaCl; ERN Laboratories, Barcelona, Spain) and administered subcutaneously (s. c.). The dose of naloxone was 15 μg/kg and was injected in volumes of 1 mL/kg of body weight. This dose was selected given that it has been reported to evoke aversive emotional symptoms of opioid withdrawal and, consequently, elicit significant place aversion in morphine dependent animals but not in controls, and reduced physical ones [31–33].

2.3. Behavioural procedures

2.3.1. Induction of morphine dependence

Morphine dependence was induced by subcutaneous (s.c.) implantation of 2 morphine pellets in the interscapular area of the animals under isoflurane anesthesia. This method has been proven to induce dependence within the next 24 h following the surgical procedure and to maintain stable the plasmatic levels of morphine for 15 days [34–36]. Rats were randomly divided into two groups: one of them had lactose pellets implanted and the other group was surgically intervened with morphine pellets.

2.3.2. Conditioning apparatus

Conditioning apparatus (Panlab, Barcelona, Spain) consisted of a box separated in two same-size chambers (40 × 13 × 45 cm) connected through a rectangular corridor (25 × 13 × 45 cm). Both chambers show different visual patterns on the walls (black dots or grey stripes), different colour and texture of the floor (black or grey, smooth, or rough, respectively). The combinations were: (A) black-dotted walls, smooth black floor; and (B) black-stripped walls, rough grey floor. Walls in the corridor were transparent, which minimized the time that the animals stay in it. The position of the animal during the test and the number of entries in every chamber were detected through transduction technology and the program PPCWIN (Panlab). Experimental protocol consisted of three phases: pre-conditioning, conditioning, and test. Since chronic morphine treatment reduces weight gain because of a lower caloric intake [34,35,37] animal weight was measured every day to check that morphine was properly released from the pellets.

2.3.3. Conditioning place aversion protocol (CPA)

Briefly, CPA protocol consisted of three phases (Fig. 1A). Firstly, during the pre-conditioning phase, rats were allowed to explore freely the conditioning apparatus to test and exclude those with natural preference to any chamber. Secondly, in the conditioning phase, morphine withdrawal was induced by administration of naloxone and animals were confined to one of the compartments, which allowed them to associate the negative symptoms of withdrawal with that environment. In the last stage, animals were again allowed to freely explore the apparatus and to test whether they retrieved the environmental memories associated with the abstinence syndrome and, therefore, avoided the withdrawal-paired chamber.

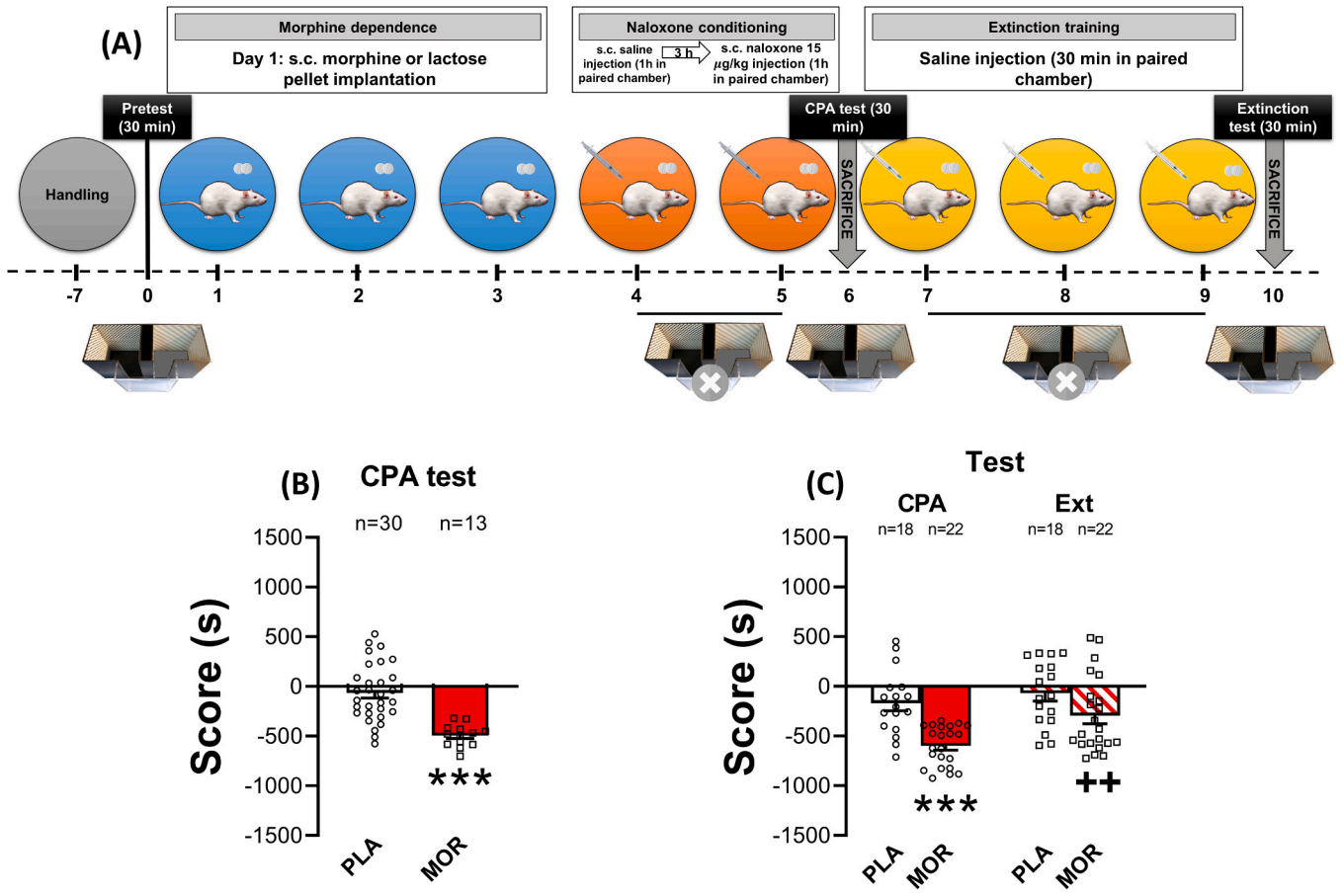

Fig. 1. (A) Experimental design. After seven days of handling, on day 0 rats were placed in the central corridor and allowed to explore the apparatus freely for 30 min (pre-test). On day 1, rats were implanted with 2 placebo or morphine pellets and were let to recover for 3 days. On day 4, for each rat, one chamber was randomly chosen to be paired with naloxone and the other chamber with saline (conditioning sessions). CPA test was conducted on day 6, exactly as in the preconditioning phase, and a set of animals were sacrificed. After the test, and for 3 days, another set of animals was injected with saline and confined in both chambers. On day 10, rats were tested as in CPA test (extinction test). (B) Scores after CPA test. * **$P < 0.001$ versus the placebo control animals (Student's t test; $t_{(41)} = 5.175$; $P < 0.0001$). (C) CPA and extinction scores. * **$P < 0.001$ versus the placebo control animals; $^{++}P < 0.01$ versus morphine-CPA (two-way ANOVA with Sídák's *post-hoc* analysis).

2.3.4. *Pre-conditioning phase*

In this phase (day 0), animals were placed in the central corridor and were free to explore the apparatus for 30 min (pre-test). Animals that showed natural preference or aversion for one of the chambers (more than 60% of the time and less of the 40% of the time of the session, respectively) were discarded. One chamber was randomly chosen for the animal to associate it with withdrawal syndrome to morphine, and the other was where the animal was placed after saline administration (Fig. 1A).

2.3.5. *Conditioning phase*

In this phase guillotine doors blocked access from both compartments to the central corridor. Three days after pellets implantation, animals received a s.c. injection of saline and were confined in their previously assigned chamber for 1 h. Three hours after the saline administration, rats received a dose of naloxone s.c. to provoke an emotional withdrawal syndrome and were placed in the withdrawal syndrome opposite compartment for 1 h. This process was repeated for 2 consecutive days for control and morphine-treated rats (Fig. 1A).

2.3.6. *CPA test*

CPA test was performed the following day after the last conditioning session, similarly to the pre-conditioning phase: animals had 30 min to explore freely both chambers. Sixty min after the CPA test started, part of the morphine-dependent animals (morphine-CPA; MOR-CPA) and part of the controls (placebo-CPA; PLA-CPA) were sacrificed by transcardiac perfusion or decapitation. Resulting scores of the difference between the time that animals stayed in the compartment associated with morphine-withdrawal during the CPA test and that during the pre-conditioning test were obtained (Fig. 1A).

2.4. *Extinction of the CPA protocol*

2.4.1. *Extinction training phase*

In this phase, guillotine doors blocked access from both chambers to the central corridor. After CPA testing, another group of morphine dependent rats and their controls followed the extinction conditioning protocol of Myers et al. [33] with several modifications. The next day after CPA test, rats were injected with saline and placed in the chamber previously assigned to saline for 30 min. After this period, rats were put back to their cages. Three h after the first injection, rats were injected again with saline and placed in the opposite chamber, previously associated with withdrawal syndrome, for 30 min. This process was repeated for 3 days.

2.4.2. *Extinction of the CPA test*

Extinction test was carried out similarly to the pre-conditioning and CPA tests. Control (Placebo-Extinction; PLA-EXT) and morphine-treated (Morphine-Extinction; MOR-EXT) rats were free to explore both compartments for 30 min. Sixty min after starting the test, animals were

sacrificed through transcardiac perfusion or decapitation. Resulting scores of the difference between the time animals stayed in the chamber associated with morphine-withdrawal during the extinction test and the pre-conditioning test were calculated (Fig. 1A).

2.5. Behavioural groups

Experiment 1: induction of morphine dependence and naloxone-induced aversion to the environment.

For the CPA induction, a total of 43 rats were used: 30 of them were surgically implanted with two lactose pellets and 13 of them with two steady-release morphine pellets to induce morphine dependence. Both groups were conditioned with naloxone and re-exposed to both compartments during CPA test. After this procedure, 5–6 brains were processed for immunostaining protocols and 4–6 were used for RT-qPCR.

Experiment 2: extinction of naloxone-induced aversion to the environment.

Another set of animals followed the previously described procedure and was also subjected to extinction training. Eighteen rats were surgically intervened with lactose pellets and 22 animals were implanted with morphine pellets. After extinction training and test, 5–6 rat brains of each group were processed for immunofluorescence assays and 4–6 were extracted for RT-qPCR analyses.

2.6. Sample processing

For immunostaining procedures, rats were transcardiacally perfused: first, they were anesthetized with a sublethal dose of pentobarbital (100 mg/kg intraperitoneal; i. p.) and later were perfused with 250 mL of saline 0.9% followed by 500 mL of fixative solution (paraformaldehyde 4% in borate buffer 0.1 M pH 9.5). Then, fixed brains were extracted and kept in fixative solution with sucrose to preserve the tissue (paraformaldehyde 4% and sucrose 30% in borate buffer 0.1 M pH 9.5) for 3 h. For molecular assays, rats were decapitated, brains were rapidly removed and stored immediately at − 80 °C until use for quantitative real-time PCR.

2.7. Immunofluorescence assay

To identify the brain regions of interest (BLA, DG, CA1 and CA3), Paxinos and Watson atlas [38] was used. Four to five animals of each group were used for immunostaining. Sections were washed with PBS and an antigen retrieval technique was carried out. To accomplish this, sections were exposed to citrate buffer (citric acid 10 mM in 0.05% of Tween-20, pH 6.0, 90ºC; 2 times for 10 min each). Unspecific bindings were blocked with BSA solution (5% in 0.3% of Triton-X-100 in PBS for 90 min, RT). Afterwards, sections were incubated for 72 h at 4 ºC with gentle agitation with rabbit polyclonal anti phospho(p)-Brd4 (1:1000, ABE1453, Merck Millipore, MA, USA). After this, sections were washed in PBS and incubated with polyclonal anti-sheep antibody conjugated with Alexa Fluor 555 (A-31572; 1:1000, Invitrogen, Massachusetts, USA) for 4 h at 4 ºC. After this first phase, sections were washed and reblocked with BSA solution and were incubated with rabbit polyclonal biotin-conjugated anti H4K5ac (NB21–2024B; 1:1000, Novus Biologicals, Centennial, CO, USA) for 24 h at 4 ºC with gentle agitation. The next day, brain samples were washed again and were incubated with streptavidin conjugated with Alexa Fluor 647 (S32357; 1:400, Thermo Fisher Scientific, Waltham, MA, USA) for 1 h at RT. Sections were washed again and mounted with ProLong Diamond antifade with DAPI (P36962, Thermo Fisher Scientific).

2.8. Immunoreactivity quantification analysis

Images were captured by using a Leica epifluorescence microscope (Leica DM4 B) connected to a video camera (Leica Microsystems, Barcelona, Spain; DFC7000 T). Light emission from specific labelling was obtained through RHO filter cube (Leica Microsystems; excitation range: 541–551 nm; dichromatic mirror: 560 nm; emission filter: 565–605 nm) and Y5 filter cube (Leica Microsystems; excitation range: 590–650 nm; dichromatic mirror: 660 nm; emission filter: 662–738 nm). Time exposure and settings for all nuclei were constant through experimental groups and images were captured at 20X magnification. All sections were quantified by a blinded investigator. The mean grey value was measured for each channel separately by using FIJI software v. 2.1.0/1.53c (NIH ImageJ, Bethesda, MD, USA). A minimum of three sections of each animal were evaluated and a mean value for each animal was then calculated.

2.9. Confocal analysis and 3D rendering

Confocal images were obtained by using a confocal microscope Leica TCS SP8 (Leica Microsystems, Barcelona, Spain) and LAS X (Leica Microsystems) processing software. Images from the nuclei were captured from low magnification to high magnification (10X to 63X). Confocal images were obtained using 405 nm excitation for DAPI, 555 nm excitation for Alexa Fluor 555 and 647 nm excitation for Alexa Fluor 647. Emitted light was detected in the range of 405 – 490 nm for DAPI, 555 – 640 nm for Alexa Fluor 555 and 647 – 755 nm for Alexa Fluor 647. Every channel was captured separately to avoid spectral cross-talking. The confocal microscope settings were stablished and maintained by local technicians for optimal resolution. Three-dimensional reconstructions of the z-stacks of confocal images were rendered in Imaris software (Bitplane Scientific Software, Zurich, Switzerland).

2.10. Quantitative colocalization

To evaluate whether the degree of coexpression and colocalization of the tandem p-Brd4/H4K5ac was altered after CPA and extinction memory retrieval, confocal images (z-stacks) were assessed through quantitative correlation and colocalization in each nucleus were estimated by using Pearson's correlation coefficient (PCC) and Manders' overlap coefficients, respectively (MOC; M1 and M2) [39]. Colocalization analysis was performed in images in which Costes' thresholding method was applied for each channel through Imaris Software [40]. Two to three images per animal were analysed.

PCC was used for measuring the correlation of the intensity distributions between channels (values range: −1.0 to 1.0), according to the formula:

$$R_r = \frac{\sum_i (S1_i - S1_{aver}) \cdot (S2_i - S2_{aver})}{\sqrt{\sum_i (S1_i - S1_{aver})^2 \cdot \sum_i (S2_i - S2_{aver})^2}}$$

Where *S*1 represents the signal intensity of pixels in the channel 1 and *S*2 represents signal intensity of pixels in the channel 2; $S1_{aver}$ and $S2_{aver}$ reflect the average intensities of these respective channels. MOC represents the fraction of one protein that co-localizes with a second protein and is a measure of the overlapped fraction of each signal. Its values are in the range 0–1.0. For two probes (*S1* and *S2*), these coefficients are calculated as:

$$M1 = \frac{\sum_i S1_{i,coloc}}{\sum_i S1_i}$$

$$M2 = \frac{\sum_i S2_{i,coloc}}{\sum_i S2_i}$$

Where *M1* is the fraction of *S1* in compartments containing *S2* and *M2* is the fraction of *S2* in compartments containing *S1*.

2.11. Cell counting

The image stack at 63X from confocal microscope was processed to obtain the maximum intensity projection (MAP) through Imaris Software. From raw MAP images, the "spots creation" module allowed us to recognize each immunofluorescence signal and to count them automatically. Minimum diameter recognition was set according to neuron size (8 μm). Spot distance between channels was calculated and those in which distance was less than the radius (4 μm) was visually overlapping and considered positive for both channels.

2.12. RNA extraction and quantitative real-time PCR (RT-qPCR)

One punch from each nucleus (BLA, DG, CA1 and CA3) was extracted and homogenized with Trizol (Qiagen, Valencia, CA, USA). Total RNA was extracted with the Qiagen RNeasy Lipid Tissue Mini Kit (Qiagen). For this purpose, manufacturer's instructions were followed. RNA concentration and purity were measured in a spectrophotometer NanoDrop (Thermo Scientific). Purity measurements (A_{260}/A_{280}) yielded ratios comprising 1.6–2.0. One hundred ng of RNA was used for cDNA synthesis with the High-Capacity cDNA Reverse Transcription (Applied Biosystems, Waltham, MA, USA). To avoid RNA degradation, RNAase inhibitors (Applied Biosystems) were used at a final concentration of 1.0 U/μL. Retrotranscription was performed in Veriti Thermal Cycler (Applied Biosystems) and parameters were set accordingly to the manufacturer's optimized configuration: 10 min at 25 ºC, 2 h at 37 ºC and 5 min at 85 ºC. qPCR primers were designed with Primer3 software (Whitehead Institute, Cambridge, MA, USA). Primers (Table 1; Integrated DNA Technologies, Leuven, Belgium) were used in qPCR with SybrGreen qPCR Master Mix (Applied Biosystems). qPCR experiments were carried out in the Fast Real-Time PCR System apparatus (Applied Biosystems). Forty PCR cycles were performed according to the supplier's guidelines: 2 min at 50 ºC, 10 min at 95 ºC (holding stage), 15 min at 95 ºC and 1 min at 60 ºC (cycling stage). DEPC-treated water combined with SybrGreen Master Mix was used as internal negative control in PCR templates. Amplifications were carried out in triplicate and C_q variations among triplicates were not greater than 0.5 cycles. Relative expression of target genes was determined by the ΔΔCT method. *Actb* (β-actin) was used as a reference gene for normalization.

2.13. Data analysis

Placebo and morphine groups within tests were analysed through paired Student's *t* test for behavioural data and unpaired Student's *t* test for molecular data. Behavioural data across tests were analysed by using repeated measures two-way analysis of variance (ANOVA) followed by a *post-hoc* Sidak's test to determine specific group differences. Molecular data across tests were analysed by non-parametric ANOVA (Kruskal-Wallis) followed by Dunn's *post-hoc* test. Molecular results that revealed statistical differences were subjected to Cohen's *d* test to measure the effect size of the treatment when compared with their control group. All statistical analyses were performed using GraphPad Prism 9 (GraphPad Software Inc., San Diego, CA, USA). Data are presented as mean ± standard error of the mean (SEM). Significance was set at $P < 0.05$ for all statistical tests. Absence of outliers (ROUT Method; Q = 1%) was confirmed.

3. Results

No significant differences ($t_{(92)} = 0.7430$; P=0.4594; Student's *t* test) were found in the weight gained by animals in the 5 days previous to pellets implantation and that were posteriorly implanted with placebo (27.4 ± 1.129 g; n = 48) or morphine (28.54 ± 1.696 g; n = 46) pellets. By contrast, and according to previous data [35,37,41,42] Student's *t* test ($t_{(92)} = 8.076$; $P < 0.0001$) showed that weight gain in rats subjected to morphine dependence induction, from the day of morphine implantation (day 1) to the first day of conditioning (day 4) was lower (7.217 ± 1.521 g) than that in the placebo group (22.50 ± 1.144 g).

3.1. Motivating effects of the context associated with morphine withdrawal and its suppression by extinction training

3.1.1. Aversive behaviour induced by opiate withdrawal syndrome

We trained rats on a CPA paradigm (Fig. 1A). We chose CPA paradigm because is a highly sensitive, long lasting learning model for measurement of the aversive negative affective component of opiate withdrawal [6], and it develops through associative learning and requires synaptic plasticity [10]. Rats made dependent on morphine for three days and tested for aversion to the naloxone-paired chamber (CPA test) showed a significantly lower score than that of placebo control animals ($t_{(41)} = 5.175$; $P < 0.0001$; Fig. 1B), thus indicating that the dose of naloxone administered for the conditioning elicited the aversive emotional state characteristic of morphine withdrawal in opiate-dependent rats but not in controls. Some rats of both groups were sacrificed after the CPA test for the molecular study.

3.1.2. Extinction training suppressed the aversive behaviour induced by morphine withdrawal

Since extinction therapy has been proposed to reduce the motivational impact of drug-associated cues to prevent relapse [15], other groups of rats were not sacrificed after the CPA test but followed a reconditioning procedure to extinguish the previously acquired CPA to the morphine withdrawal-associated chamber (Fig. 1C). Two-way ANOVA analysis of the scores (for details, see Table S1) revealed a significant influence of the pharmacological treatment (placebo or morphine pellets) and the behavioural procedure (CPA or extinction). Sídák's multiple comparisons test revealed that that morphine-dependent rats showed extinction, since the score was significantly higher than their previous CPA score. Thus, the reconditioning procedure was effective to suppress the CPA induced by morphine withdrawal.

3.2. H4K5ac and p-Brd4 regulation in the BLA and hippocampus during conditioned-place aversion and after the extinction phase

To determine whether histone acetyl-lysine is altered by reactivation of aversive affective memories (CPA) and/or after the extinction training, H4K5ac immunoreactivity (IR) was measured in the BLA and in

Table 1
Primers used for RT-qPCR experiments.

Gene	Gene accession number	Forward	Reverse
Actb	ENSRNOT00000116486.1	5' –CCCTAGACTTCGAGCAAGAGATG – 3'	5' – CCACAGGATTCCATACCCAGG – 3'
Smarcc1	ENSRNOG00000020804.8	5' – GGATGCGCCTACCAATAAAA – 3'	5' – ACTTGTAAGCAGCCCCAAGA – 3'
Arc	ENSRNOG00000043465.4	5' – CCCCCAGCAGTGATTCATAC – 3'	5' – CAGACATGGCCGGAAAGACT – 3'
Bdnf	ENSRNOG00000047466.3	5' – AAACGTCCACGGACAAGGCA – 3'	5' – TTCTGGTCCTCATCCAGCAGC – 3'
Creb	ENSRNOG00000013412.8	5' – TCAGCCGGGTACTACCATTC – 3'	5' – TTCAGCAGGCTGTGTAGGAA – 3'
Egr-1	ENSRNOG00000019422.5	5' – CACCTGACCACAGAGTCCTTTT – 3'	5' – ACCAGCGCCTTCTCGTTATT – 3'
Fos	ENSRNOG00000008015.6	5' – ACAGCCTTTCCTACTACCATTCCC – 3'	5'- CTGCACAAAGCCAAACTCACCTGT – 3'
Nfkb	ENSRNOG00000023258.7	5' - GCAAACCTGGGAATACTTCATGT GACTAAG – 3'	5' - ATAGGCAAGGTCAGAATGCACCAGAAGTCC – 3'

different parts of the hippocampus: DG, CA1 and CA3 (Fig. 2). Our study addressed the changes of H4K5ac IR (measured as the mean grey value) as a mark of actively transcribed genes associated with memory formation. As depicted in Fig. 2B, our study revealed that, following retrieval of Pavlovian cued morphine-withdrawal associations (CPA), there was not significant elevation of H4K5ac in the BLA compared with the control (Student's *t* test: $t_{(8)} = 1.681$; P=0.1313), whereas in the hippocampal DG ($t_{(8)} = 2.795$; P=0.0234; Cohen's $d = 1.77$), CA1 ($t_{(8)} = 3.4472$; P=0.0084; Cohen's $d = 2.20$) and CA3 ($t_{(8)} = 3.224$; P=0.0122; Cohen's $d = 1.66$) areas there was a significant elevation of H4K5ac IR (Fig. 2C,D,E, respectively). To compare the data of animals that showed CPA vs. animals that extinguished it, we used Kruskal-Wallis ANOVA followed by Dunn's *post-hoc* test. ANOVA for H4K5ac in the BLA failed to show differences within groups ($H = 4.701$; P=0.195). By contrast, ANOVA analysis manifested differences within groups in the DG ($H = 9.657$; P=0.0217) in the CA1 ($H = 12.47$; P=0.0059) and the CA3 ($H = 10.68$; P=0.0136). The *post-hoc* test indicated that after the extinction test there was a significant reduction in the H4K5ac IR in DG (Cohen's $d = -4.31$), CA1 (Cohen's $d = -4.03$) and CA3 (Cohen's $d = -5.11$; Fig. 2C, D, E) in morphine-dependent animals regarding the CPA test. Representative images are shown in Fig. 2J-M (BLA), N-Q (DG), R-U (CA1) and V-Y (CA3).

Since H4K5ac mark has shown to be a target of Brd4 [43,44], we next sought to determine in the same animals whether activated Brd4 (p-Brd4) IR changes paralleled with H4K5ac expression after the re-exposure to the withdrawal-paired environment (CPA) and after the extinction training. As shown in Fig. 2F-I, the CPA test caused a significant increase in p-Brd4 in the four areas studied: BLA ($t_{(8)} = 3.668$; P=0.0063; Cohen's $d = 2.32$); DG ($t_{(8)} = 3.471$; P=0.0084; Cohen's $d = 2.20$); CA1 ($t_{(8)} = 5.086$; P=0.0009; Cohen's $d = 3.22$); and CA3 ($t_{(8)} = 3.461$; P=0.0086; Cohen's $d = 2.19$). To compare the data of animals that showed CPA vs. animals that extinguished it, we used non-parametric ANOVA followed by a Dunn's multiple comparisons *post-hoc* test. After the extinction test, ANOVA for p-Brd4 in the BLA did not show any significant effects ($H = 5.37$; P=0.1466). In the DG, ANOVA showed differences within groups ($H = 10.94$; P=0.0121). Additionally, both in the CA1 and CA3, ANOVA for p-Brd4 showed main effects (CA1: $H = 10.92$; P=0.0122; CA3: $H = 8.086$; P=0.443).

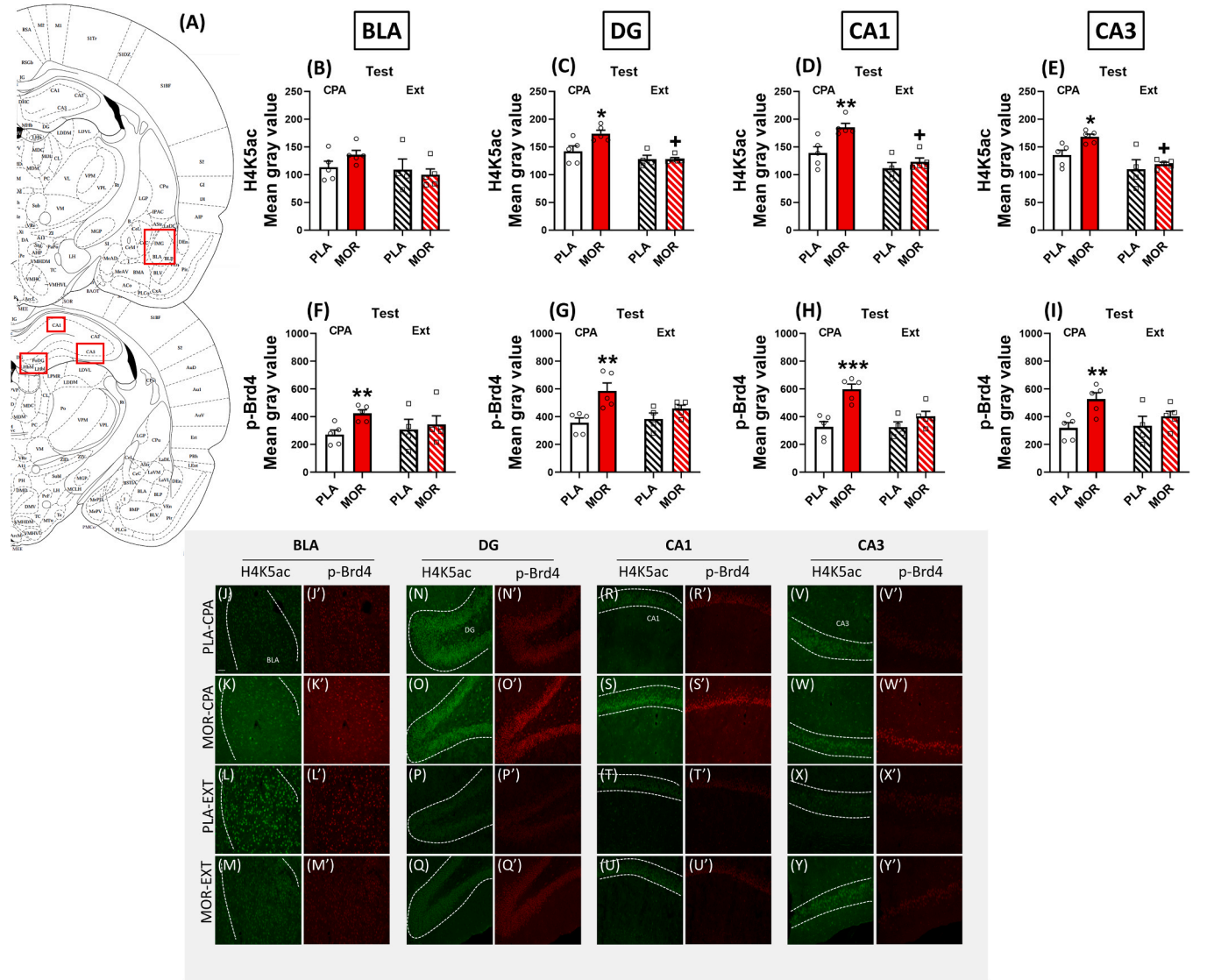

Fig. 2. (A) Schematic illustrations of coronal sections showing the BLA and the hippocampus (DG, CA1 and CA3) (modified from Paxinos and Watson 2007). Quantitative H4K5ac IR and p-Brd4 IR in the BLA (B, F), DG (C, G), CA1 (D, H) and CA3 (E, I) after conditioned place aversion (CPA) paradigm and after the post-extinction (Ext) CPA test. *P < 0.05, * *P < 0.001, * **P < 0.0001 versus CPA-PLA group (Student's t test; for details, see Table S2). $^{+}$P < 0.05 versus MOR-Ext (Kruskal-Wallis ANOVA with Dunn's *post-hoc* analysis; n = 4–5 for each group). (J-I') Representative confocal microphotographs showing coronal section of rats immunostained in: green (H4K5ac) and red (p-Brd4). Scale bar, 25 μm.

However, Dunn's *post-hoc* test did not reveal any differences across experiments. Representative images are shown in Fig. 2J'-M', N'-Q', R'-U' and V'-Y'.

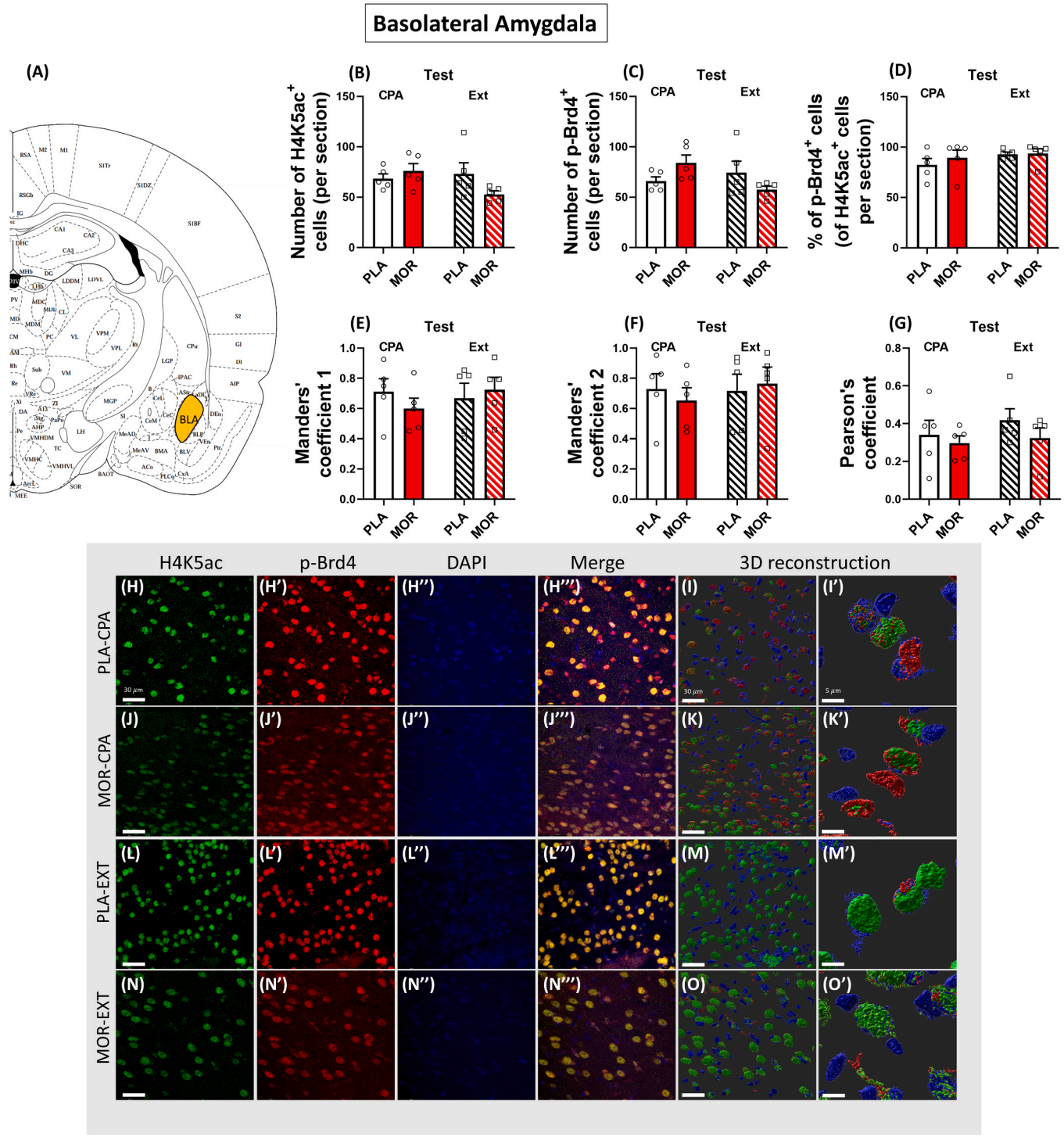

Fig. 3. Number of H4K5ac- (B) and p-Brd4-positive neurons (C), and percentage of p-BRD4 expressing H4K5ac (D) in the BLA did not change after the CPA test nor after the extinction test (for details, see table S3). The analysed region within the BLA is schematically illustrated in (A). Representative confocal images in the BLA of H4K5ac (green; H-N), p-Brd4 (red; H'-N') and DAPI (nuclear stain, blue; H''-N''). Merged images are shown in (H'''-N'''; H4K5ac/p-Brd4). Colocalization is shown by yellow/orange neurons in the nucleus of merged images of H4K5ac/p-Brd4. Scale bars, 30 μm. (I-O, scale bars 30 μm; I'-O', scale bars 5 μm) Three-dimensional reconstructions of nuclei expressing H4K5ac/p-Brd4 in the BLA after different treatments. (E-G) Quantitative colocalization was performed, and several colocalization parameters were determined [Pearson's coefficient, Manders' coefficient 1-the fraction of objects in channel A (H4K5ac) colocalized with objects in channel B (p-Brd4) and Manders' coefficient 2-vice versa]. Results are expressed as mean ± SEM. N = 5 animals per group.

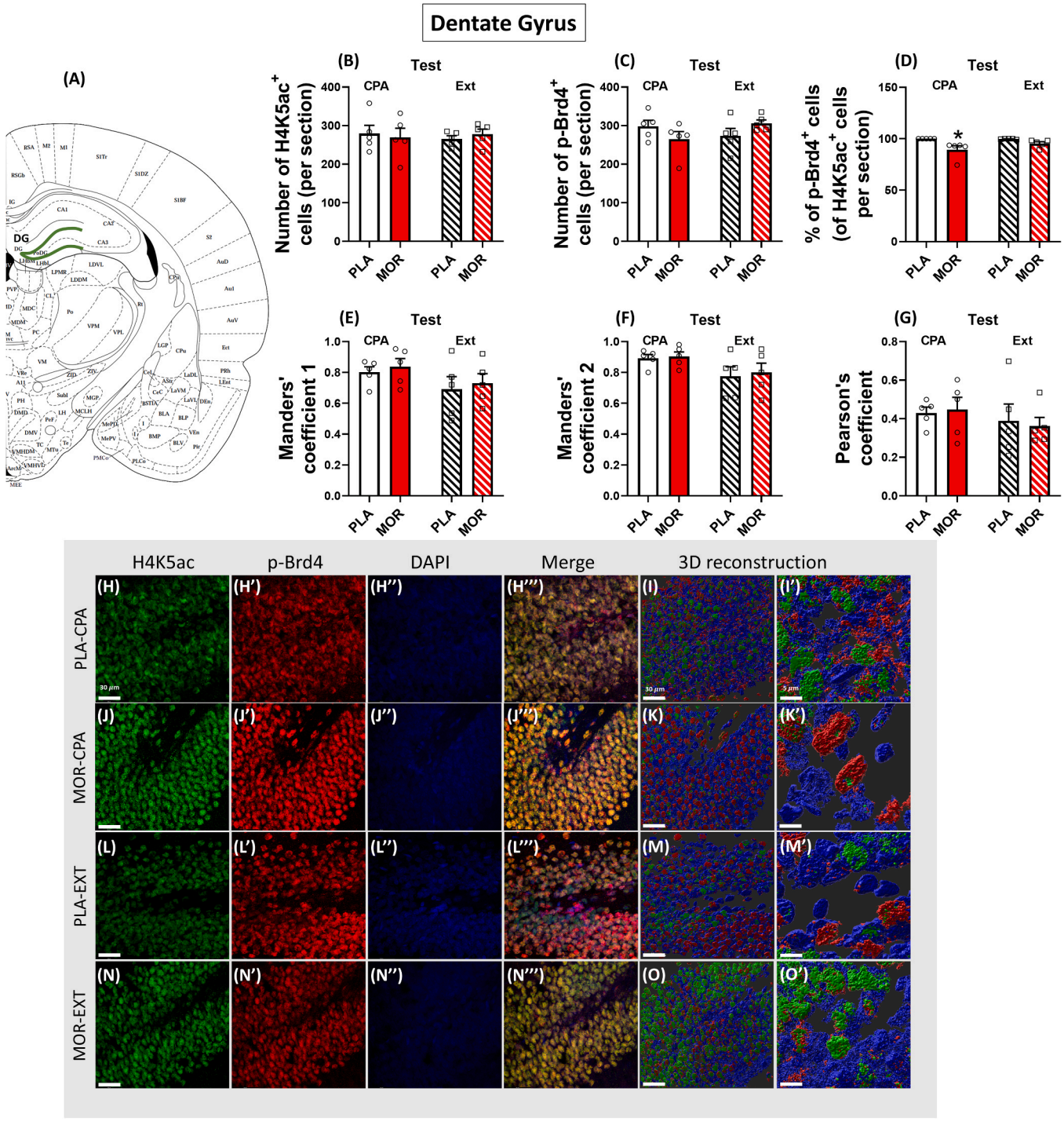

Fig. 4. Number of H4K5ac- (B) and p-Brd4-positive neurons (C), and percentage of p-BRD4 expressing H4K5 (D) in the DG after the CPA test and after the extinction test. Results are shown as mean ▫ SEM. *P < 0.05 versus the PLA-CPA group (for details, see table S4). The analysed region within the DG is schematically illustrated in (A). Representative confocal images in the DG of H4K5ac (green; H-N), p-Brd4 (red; H'-N') and DAPI (nuclear stain, blue; H''-N''). Merged images are shown in (H'''-N'''; H4K5ac/p-Brd4). Colocalization is shown by yellow/orange neurons in the nucleus of merged images of H4K5/p-Brd4. Scale bars, 30 μm. (I-O, scale bars 30 μm; I'-O', scale bars 5 μm) Three-dimensional reconstructions of nuclei expressing H4K5ac/p-Brd4 in the BLA after different treatments. (E-G) Quantitative colocalization was performed, and several colocalization parameters were determined [Pearson's coefficient, Manders' coefficient 1-the fraction of objects in channel A (H4K5ac) colocalized with objects in channel B (p-Brd4) and Manders' coefficient 2-vice versa]. Results are expressed as mean ± SEM. N = 5 animals per group.

3.3. Determination of H4K5ac-IR and p-Brd4-IR cell number and quantitative colocalization analysis in the BLA and hippocampus during conditioned-place aversion and after the extinction phase

3.3.1. Immunohistochemical approach for the determination of H4K5ac, p-Brd4 and H4K5ac-positive neurons expressing p-Brd4

To extend our results, we focused on the effects of CPA and extinction training on H4K5ac- and p-Brd4-cell number as well as on number of neurons co-expressing H4K5ac and p-Brd4 in the BLA and in the hippocampus. As shown in Fig. 4B, no significant changes were detected for H4K5ac-positive neurons in the BLA after the CPA test (Student's *t* test: $t_{(8)} = 0.8749$; P=0.4071). Representative images are shown in Fig. 3H-N. Subsequently, we investigated whether CPA produced changes in the number of p-Brd4-positive neurons in the BLA. We did not identify significant differences ($t_{(8)} = 2.0430$; P=0.0753) with respect to control rats, as depicted in Fig. 3C. Representative images are shown in Fig. 3H'-N'. In the present study we confirmed the co-localization of H4K5ac-with p-Brd4-positive neurons in the BLA, although no changes ($t_{(8)} = 0.7226$; P=0.4905) were detected after the CPA (Fig. 5D). Double labelling experiments showed that H4K5ac-positive was colocalized with p-Brd4-positive neurons for all the treatments, as shown in Fig. 5H'''-N'''. Three-dimensional reconstruction of H4K5ac-positive neurons expressing p-Brd4 is shown in Fig. 5I-O'. To compare the data of animals that showed CPA vs. animals that extinguished it, we used Kruskal-Wallis ANOVA. ANOVA failed to exhibit effects for H4K5ac- ($H = 6.973$; P=0.0728), and p-Brd4-positive neurons ($H = 7.262$; P=0.0640) and the number of H4K5ac-positive neurons expressing p-Brd4 in the BLA ($H = 1.897$; P=0.594; Fig. 3B-D).

The same study was conducted in the DG, and similar results were observed. We did not identify significant differences in the number of either H4K5ac-positive ($t_{(8)} = 0.3198$; P=0.7573) or p-Brd4-positive neurons ($t_{(8)} = 1.3420$; P=0.2165) after CPA, as shown in Fig. 6B and C, respectively. As depicted in Fig. 6D, a small but significant ($t_{(8)} = 2.796$; P=0.0234) decrease in the number of H4K5ac-positive neurons expressing p-Brd4 was observed after the CPA test. Representative images are shown in Fig. 4H-N and H'-N'. Double labelling experiments showed that H4K5ac-positive were highly colocalized with p-Brd4-positive neurons for all the treatments, as shown in Fig. 4D and H'''-N'''. Three-dimensional reconstruction of H4K5ac-positive neurons expressing p-Brd4 is shown in Fig. 4I-O'. Kruskal-Wallis ANOVA for the number of H4K5ac-positive ($H = 0.7338$; P=0.8640), p-Brd4-positive neurons ($H = 4.764$; P=0.1899) failed to exhibit main differences within groups. However, ANOVA analysis revealed differences ($H = 16.44$; $P < 0.001$) in the number of H4K5ac-positive neurons expressing p-Brd4 in the DG, due to the small decrease after CPA in morphine-dependent animals (P=0.003; Cohen's $d = -1.77$; Fig. 4B-D).

Then we focused on the effects of CPA and extinction training on H4K5ac- and p-Brd4-cell number as well as on number of neurons co-expressing H4K5ac and p-Brd4 in the CA1 and CA3 hippocampal areas. The CPA test did not cause significant changes in the number of H4K5ac- or p-Brd4-positive neurons either in the CA1 (H4K5ac: $t_{(8)} = 0.8586$; P=0.4156; Fig. 7B; p-Brd4: $t_{(8)} = 0.4064$; P=0.6951; Fig. 5C) or in the CA3 (H4K5ac: $t_{(8)} = 0.9030$; P=0.0935; Fig. 7P; pBrd4: $t_{(8)} = 1.4210$; P=0.1931; Fig. 5Q). On the other hand, there was a small but significant ($t_{(8)} = 2.409$; P=0.0426; Cohen's $d = 1.53$) increase in the number of H4K5ac-positive neurons expressing p-Brd4 after the CPA test

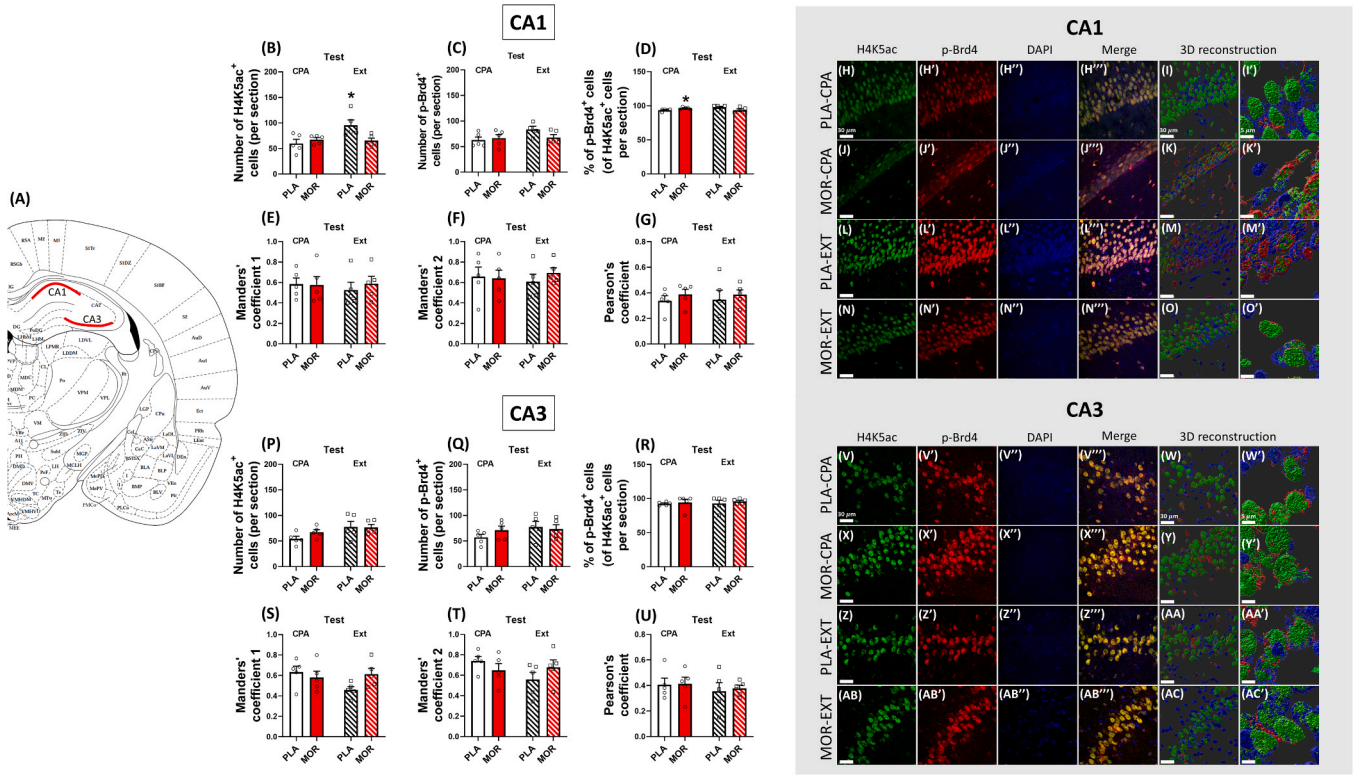

Fig. 5. Number of H4K5ac- and p-Brd4-positive neurons, and percentage of p-Brd4 expressing H4K5ac in the CA1 (B-D) and CA3 (P-R) after the CPA test and after the extinction test. Results are shown as mean ± SEM. N = 4–5 per each group. *P < 0.05 versus the PLA-CPA-group (Kruskal-Wallis ANOVA with Dunn's *post-hoc* analysis). The analysed regions within the CA1 and CA3 are schematically illustrated in (A). Representative confocal images in the CA1 of H4K5ac (green; H-N), p-Brd4 (red; H'-N') and DAPI (nuclear stain, blue; H''-N'') and in the CA3 (V-AB for H4K5, green; V'-AB' for p-Brd4, red; and V''-AB'' for DAPI, blue). Merged images are shown in H'''-N''' for CA1 and V'''-AB''' for CA3; H4K5ac/p-Brd4). Colocalization is shown by yellow/orange neurons in the nucleus of merged images of H4K5ac/p-Brd4. Scale bars, 30 μm. (I-O for CA1 and W-AC for CA3, scale bars 30 μm; I'-O' for CA1 and W'-AC' for CA3, scale bars 5 μm) Three-dimensional reconstructions of nuclei expressing H4K5ac/p-Brd4 in the CA1 and CA3 after different treatments. (E-G; S-U) Quantitative colocalization was performed, and several colocalization parameters were determined [Pearson's coefficient, Manders' coefficient 1-the fraction of objects in channel A (H4K5ac) colocalized with objects in channel B (p-Brd4) and Manders' coefficient 2-vice versa]. Results are expressed as mean ± SEM. N = 5 animals per group.

in CA1 but not in the CA3 ($t_{(8)} = 0.3647$; P=0.7248) (Fig. 5D and R, respectively). Representative images are shown in Fig. 5 (CA1: H-N'''; CA3: V-AB'''). Three-dimensional reconstruction of H4K5ac-positive neurons expressing p-Brd4 is shown in Fig. 5I-O' for CA1 and W-AC' for CA3. To compare the data of animals that showed CPA vs. animals that extinguished it in the CA1 and CA3, we used Kruskal-Wallis ANOVA followed by Dunn's *post-hoc* test. After the extinction test, ANOVA for the number of H4K5ac-positive cells In the CA1 showed differences within groups (H = 9.846; P=0.0199). Unexpectedly, an increase of H4K5ac-positive neurons was observed in the control group after the extinction test regarding the same group after the CPA test (P=0.0299; Fig. 5B). ANOVA for the number of p-Brd4-positive neurons (H = 4.86; P=0.1823) and the percentage of H4K5ac-positive neurons expressing p-Brd4 in CA1 (H = 6.251; P=0.10; Fig. 5C, D) as well as for the number of H4K5ac-positive (H = 5.327; P=0.1494), p-Brd4-positive cells (H = 3.611; P=0.3066) and the percentage of H4K5ac-positive neurons expressing p-Brd4 in CA3 (H = 2.855; P=0.4145; Fig. 5P-R) failed to exhibit differences across experiments.

3.3.2. *Quantitative co-localization analysis*

Quantitative co-localization analysis was performed, and co-localization parameters and correlation were performed in the BLA, DG, CA1 and CA3. Using Manders' and Pearson's coefficients, in the present study we confirmed the co-localization of H4K5ac with p-Brd4-positive neurons in the four areas studied. Quantitative analysis for H4K5ac-p-Brd4 co-localization is shown in Fig. 3E-G (BLA), Fig. 4E-G (DG) and Fig. 5 (E-G for CA1 and S-U for CA3). As shown in Tables S2, S3, S4 and S5, no significant variation was observed in Manders' or Pearson's coefficients.

3.4. *Effects of conditioned-place aversion and extinction training on the induction of gene expression*

Since H4K5/8/12/16Ac have been shown to be markers of transcriptional activation induced by drugs of abuse such as cocaine [25], and *Smarcc1* has been proposed to crucial for chromatin remodelling [26], the influence of CPA and extinction training on the transcript of *Smarcc1* was determined. The relative levels of mRNAs are presented in Figs. 6 and 7. In the BLA, we found significant changes for *Smarcc1* mRNA after CPA ($t_{(10)} = 3.974$; P=0.0026; Cohen's $d = -2.30$; Fig. 6B). However, Kruskal-Wallis ANOVA failed to show differences across experiments (H = 6.972; P=0.073). Subsequently, the influence of CPA and extinction training on mRNA *Smarcc1* in the hippocampus was analyzed. We found that the expression of *Smarcc1* mRNA in the DG was slightly, although not significantly, reduced after CPA test ($t_{(9)} = 1.811$; P=0.1036; Fig. 7B). After the third day of extinction training, ANOVA did not reveal any differences among groups (H = 5.715; P=0.126). In the CA1, we also found a significant decrease in *Smarcc1* mRNA levels after CPA ($t_{(9)} = 2.718$; P=0.0237; Cohen's $d = -1.58$). ANOVA analysis did not showed differences across experiments on *Smarcc1* mRNA levels (H = 7.569; P=0.056). In the CA3 nuclei, no significant changes were found in the relative levels of *Smarcc1* mRNA after CPA test ($t_{(9)} = 1.172$; P=0.2713). ANOVA neither revealed any differences among groups (H = 4.041; P=0.257). To extend our results, and to assess the degree of transcriptional activation, a set of IEGs, critical for synaptic plasticity (*Arc, Egr-1*, *Fos, Creb, Bdnf* and *Nfkb*) were analyzed using quantitative real-time PCR in the four areas studied. In the BLA, *Egr-1* levels were reduced after CPA test on morphine-treated animals ($t_{(10)} = 3.386$; P=0.0069; Cohen's $d = -1.96$; Fig. 6F). We found that transcript of *Bdnf, Creb, Fos* and *Nfkb* genes were not altered in the BLA after the CPA test (Fig. 6D, E, G, H) (*Bdnf*: $t_{(10)} = 0.4227$; P=0.6814; *Creb*: $t_{(10)} = 1.044$; P=0.3211; *Fos*: $t_{(10)} = 0.4526$; P=0.6605; *Nfkb*: $t_{(10)} = 1.591$; P=0.1427). After the third day of extinction training, Kruskal-Wallis

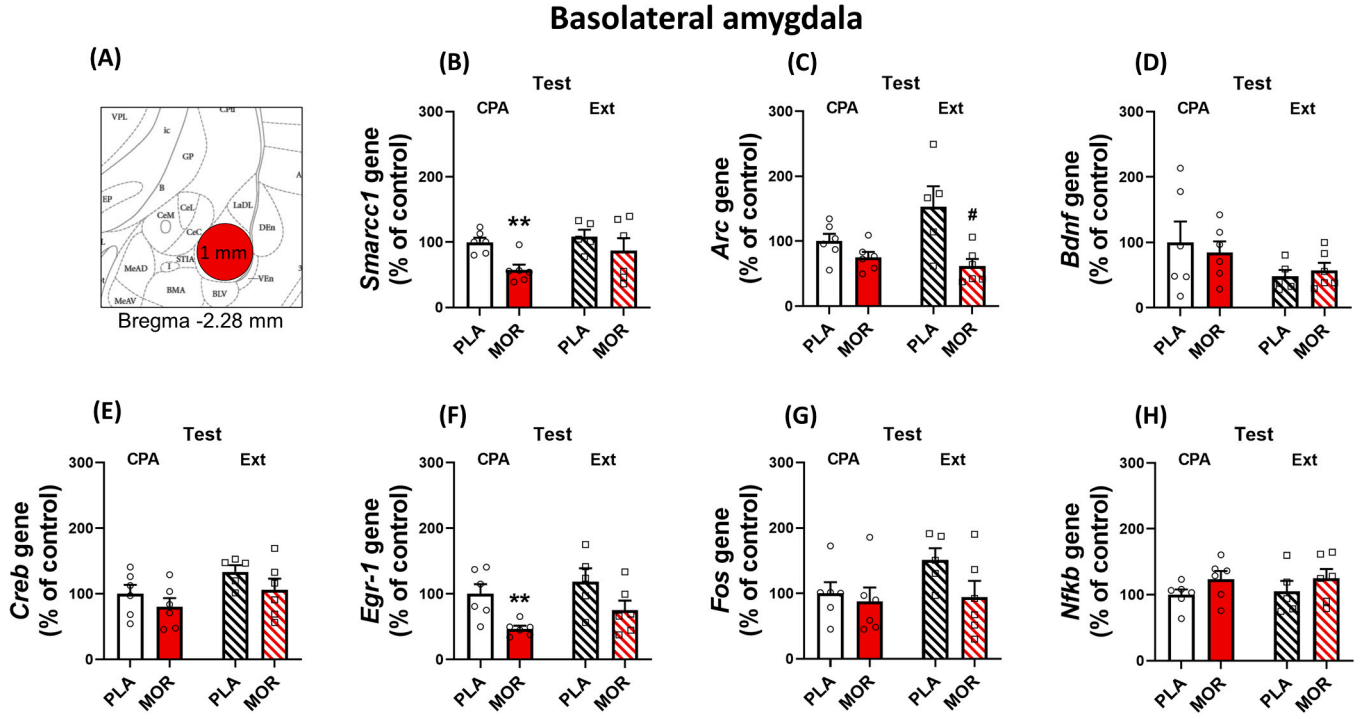

Fig. 6. mRNA levels of Smarcc1 and a set of IEGs (*Arc*, *Bdnf*, *Creb*, *Egr-1*, *Fos* and *Nfkb*) in BLA during aversive memory retrieval process and after the extinction test. Schematic representation of BLA isolation and localization modified from Paxinos and Watson atlas (2007) (A). Quantitative real-time polymerase chain reaction (qPCR) of *Smarcc1* (B), *Arc* (C), *Bdnf* (D), *Creb* (E), *Egr-1* (F), *Fos* (G) and *Nfkb* (H). * *P < 0.01 vesus placebo animals after the CPA. #P < 0.05 vs placebo animals after extinction training (Student's t test; Kruskal-Wallis ANOVA with Dunn's *post-hoc* analysis; for details, see Table S11). Results are expressed as mean ± SEM. N = 5 for PLA-EXT group. N = 6 for PLA-CPA, MOR-CPA and MOR-EXT groups.

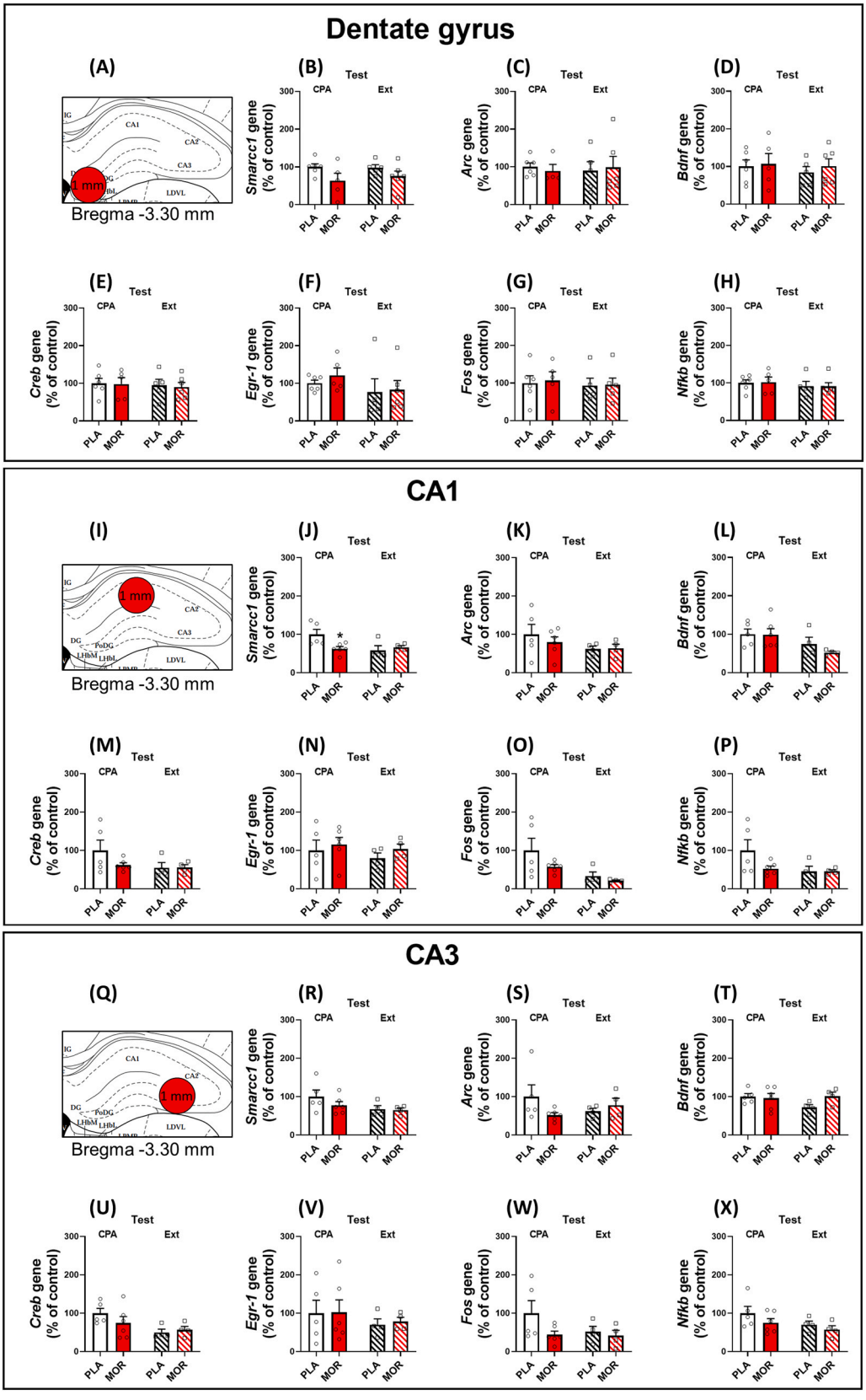

Fig. 7. mRNA levels of Smarcc1 and a set of IEGs (*Arc*, *Bdnf*, *Creb*, *Egr-1*, *Fos* and *Nfkb*) in DG (B-H), CA1 (J-P) and CA3 (R-X) during aversive memory retrieval process and after the extinction test. Schematic representations of DG, CA1 and CA3 isolation and localization modified from Paxinos and Watson atlas (2007) are shown (A, I, Q, respectively). Quantitative real-time polymerase chain reaction (qPCR) of *Smarcc1* (B, J, R), *Arc* (C, K, S), *Bdnf* (D, L, T), *Creb* (E, M, U), *Egr-1* (F, N, V), *Fos* (G, O, W) and *Nfkb* (H, P, X). *P < 0.05 vesus placebo animals after the CPA. (Student's t test). Results are expressed as mean ± SEM. [DG: n = 6 for PLA-CPA and MOR-EXT groups, n = 5 in MOR-CPA and PLA-EXT groups. CA1 and CA3: n = 5 for PLA-CPA group, n = 6 for MOR-CPA group and n = 4 for PLA-EXT and MOR-EXT groups].

ANOVA revealed differences on *Egr-1* mRNA levels (H = 10.796; P=0.013), although Dunn's test did not reach significancy. Additionally, Kruskal-Wallis ANOVA revealed a significant effect (H = 9.080; P=0.028) on *Arc* mRNA levels. *Post-hoc* analysis showed a significant decrease on *Arc* mRNA levels on morphine-dependent animals after extinction training (P=0.034; Cohen's d = −1.73). *Bdnf* (H = 2.666; P=0.446), *Creb* (H = 6.066; P=0.108), *Fos* (H = 5.327; P=0.149) and *Nfkb* (H = 3.41; P=0.333) mRNA levels remained unaltered. In the DG,

no significant changes were seen after CPA test in the set of IEGs analyzed (*Arc*: $t_{(8)} = 0.5886$; P=0.5724; *Bdnf*: $t_{(9)} = 0.2121$; P=0.8367; *Creb*: $t_{(9)} = 0.0897$; P=0.9305; *Egr-1*: $t_{(9)} = 1.074$; P=0.3106; *Fos*: $t_{(9)} = 0.2293$; P=0.8237; *Nfkb*: $t_{(9)} = 0.1508$; P=0.8834). Kruskal-Wallis ANOVA did not reveal any differences after the extinction test (*Arc*: $H = 1.276$; P=0.735; *Bdnf*: $H = 0.838$; P=0.840; *Creb*: $H = 0.395$; P=0.941; *Egr-1*: $H = 5.034$; P=0.169; *Fos*: $H = 0.983$; P=0.805; *Nfkb*: $H = 1.113$; P=0.774). In the CA1, no significant changes were seen after CPA test (*Arc*: $t_{(9)} = 0.7137$; P=0.4935; *Bdnf*: $t_{(9)} = 0.05098$; P=0.9605; *Creb*: $t_{(9)} = 1.499$; P=0.1682; *Egr-1*: $t_{(9)} = 0.4917$; P=0.6347; *Fos*: $t_{(9)} = 1.443$; P=0.1830; *Nfkb*: $t_{(9)} = 1.783$; P=0.1083). Kruskal-Wallis ANOVA revealed differences on *Bdnf* ($H = 8.075$; P=0.044) and *Fos* ($H = 10.204$; P=0.017) transcripts, although *post-hoc* analysis did not show any differencies. Nonetheless, no changes were seen in the other genes analysed (*Arc*: $H = 2.625$; P=0.453; *Bdnf*:; *Creb*: $H = 2.776$; P=0.427; *Egr-1*: $H = 2.238$; P=0.525; *Nfkb*: H= 4.127; P=0.248). In the CA3, no significant changes were seen after CPA test in the set of IEG analyzed (*Arc*: $t_{(9)} = 1.669$; P=0.1295; *Bdnf*: $t_{(9)} = 0.2325$; P=0.8214; *Creb*: $t_{(9)} = 1.164$; P=0.2742; *Egr-1*: $t_{(9)} = 0.04678$; P=0.9637; *Fos*: $t_{(9)} = 1.783$; P=0.1082; *Nfkb*: $t_{(9)} = 1.231$; P=0.2494). Likewise, Kruskal-Wallis ANOVA did not reveal any differences after the extinction test (*Arc*: $H = 3.548$; P=0.315; *Bdnf*: $H = 4.152$; P=0.246; *Creb*: $H = 5.975$; P=0.113; *Egr-1*: $H = 0.109$; P=0.991; *Fos*: $H = 2.680$; P=0.444; *Nfkb*: $H = 3.720$; P=0.293).

4. Discussion

Although most of the work examining how epigenetic modifications contribute to addiction has focused on psychostimulants like cocaine, research into opioid-induced changes to the epigenetic landscape is beginning to emerge. Nuclear chromatin structure play important roles in the nervous system, regulating, among others, neuronal activity and memory [45]. Broad research has been performed to unravel the molecular mechanisms that underlie in the processing of rewarding drug memories and their extinction [46–48]. However, less is known about the molecular processes involved in the aversive affective drug memories. In the present work, we have studied whether CPA and extinction of aversive memories associated with morphine withdrawal induce chromatin remodelling in the BLA and hippocampus, since neurochemical activity within these nuclei participate in the neuronal mechanisms mediating the negative component of opiate withdrawal [10,27,34,49].

4.1. CPA induces epigenetic regulation of H4K5ac and p-Brd4 in the BLA and hippocampus

We first analysed H4K5ac modifications in the BLA and hippocampus following aversive memory retrieval associated with morphine withdrawal. This level of acetylation mark on specific lysine residue of histone H4 was selected on the basis that H4K5ac has been proposed as one of the marks of actively transcribed genes associated with memory formation in the hippocampus [50]. We found that H4K5ac-IR significantly increased in the hippocampal areas DG, CA1 and CA3 following CPA. In addition, an increasing trend also appears in the BLA. By contrast, positive cell counting in each area remained similar across channels and conditions, meaning that, regulation of H4K5ac/p-Brd4 seemed to be provided by a modification in protein expression rather than in number of positive cells. Lack of differences in Manders' and Pearson's coefficients across experimental groups also suggested a shared regulation of the H4K5ac/p-Brd4 tandem, showing a very high correlation in overlapping signals and moderate correlation in intensity measures, thus indicating a joint control of this epigenetic tandem. Since modulation of chromatin structure through post-translational modifications of histones (e.g. acetylation) has emerged as an important mechanism for regulation of drug addiction and formation and/or consolidation of drug associated memories [51,52], present results might suggest that H4K5ac, mainly in the hippocampus, would be involved in the aversive memory of opiate withdrawal and may underlay long-lasting changes in long-term addiction memory. According to present results, disturbances of epigenetic mechanisms including histone acetylation are increasingly being recognized to play a crucial role in the development and maintenance of addictive disorders [18,52]. Thus, hyperacetylation of H3 has been observed in the NAc after chronic cocaine exposure [53]. In addition, simultaneous acetylation and phosphorylation of H3 in the rat NAc has been shown to be essential for heroin induced CPP [54]. Similarly, direct evidence of opiate-related epigenetic impairments has been shown in the post-mortem human brain from heroin users, particularly restricted to acetylation of H3K27, although nothing is known about its function in the brain during substance use disorders [55].

Epigenetic readers of acetyl-lysine histones, particularly BET bromodomain proteins, have recently emerged as important factors involved in preclinical models of substance use disorder [55,56]. BET bromodomains have been involved in cocaine reward and addiction and have been proposed as a new therapeutic avenue for the treatment of drug addiction [56,57]. However, it is unclear whether BET proteins regulate behavioural and molecular aspects of opiate addiction. The present study exhibits that activated BET protein p-Brd4-IR significantly increased in the BLA and in all the regions of the hippocampus after the recovery of negative affective memory of opiate withdrawal. Double immunofluorescence experiments also revealed that p-Brd4 immunolabeling almost completely colocalized with H4K5ac in all the studied areas. According to previous studies [58,59], present results suggest that chromatin regulation through histone acetylation and Brd4 activation appears to be a molecular mechanism for the retrieval and/or consolidation of opiate withdrawal-associated memories, which may contribute to the formation of addictive behaviour.

4.2. CPA extinction results in decreases of H4K5ac and pBrd4

Previous studies suggest that epigenetic mechanisms also have an important role in extinction of drug-seeking behaviours. Our findings show decreased H4K5ac- and p-Brd4-IR after the extinction training test. Extinction is the result of the updating of a previous memory, a form of new learning that inhibit the original memory [13]. Extinction therapy has been proposed as a nonpharmacological method for disrupting drug-associated memories to prevent the reinstatement [16,60]. Present findings showing the opposite effect of extinction test on chromatin modification compared to morphine withdrawal aversive memory retrieval may indicate that exposure of animals to the protocol of extinction might facilitate the formation of a more repressed state of chromatin in the BLA and hippocampus.

4.3. Regulation of gene transcription induced by CPA and after extinction behaviour

Accumulative evidence indicates that elevated histone acetylation levels increase the accessibility of regulatory factors to DNA and induces active gene transcription, which might be involved in neuronal and behavioural plasticity [25]. In fact, two of the best-studied sites of histones acetylation (H3K9/14 and H4K5/8/12/16) are markers of transcriptional activation [25]. On the other hand, bromodomain proteins function as epigenetic readers that recognize acetylated histone tails to facilitate the transcription of target genes [61]. Since regulation of gene transcription, in turn, may contribute to the development and maintenance of the addicted state [62], we have studied whether the observed epigenetic changes in the present work paralleled with modifications of expression of genes identified as relevant in the context of neuronal activity and neuroplasticity.

Interestingly, despite finding a common upregulated pattern in p-Brd4 and H4K5ac expression after the retrieval of aversive memories, in our work most of the set of IEGs analysed remained unchanged in BLA and hippocampus, thus pointing out that apparently these genes are

implicated neither in the retrieval of aversive drug memories nor in memory updating during the extinction process. These data might suggest that p-Brd4 enhancement under these conditions might not be sufficient to induce their transcription. Only *Arc*, and accordingly to former work of our lab [63], revealed a decrease in its transcript after extinction training in BLA, paralleling with the reduced expression levels of these epigenetic marks. Previous studies evaluated the need of, not only Brd4, but the conjunction of all BET members of the family to increase gene transcription, seeing that specific Brd4 inhibition does not fully mimic the effects of pan-BET inhibition [64]. In our work, intriguingly, we found that *Egr-1* gene was downregulated after the recall of aversive memories in the BLA, which paralleled with p-Brd4 enhancement. In this line of evidence, previous reports found that IEGs were upregulated following BET inhibition, showing an intricate regulation regarding BRD-induced transcription [65]. Notably, it has been found that, through BET inhibition, there was not any reversal of BDNF-induced enhancement in several IEGs mRNA levels, thus suggesting a secondary or late response genes disruption, but not IEGs [66]. Together, and taken into consideration that IEGs mRNA expression shows various patterns regarding half-life and stimulus associated burst in transcription [24,67], it might be possible that, in our model, recall of aversive memories could not be enough to maintain IEGs expression after 60 min following the start of free exploration. Hence, a secondary response might already be happening in response to the initial retrieval stimulus, where H4K5ac and p-Brd4 could be acting. Brd4 is known to be chromatin-bound in a paused state, and following stimuli induction, it is released through differential deacetylation, being then free to interact with its downstream regulators, such as p-TEFb, activating transcription [68]. Hence, our results might indicate that binding of p-Brd4 to marked acetylated sites on chromatin might not strictly reflect the degree of transcription activation on poised promoter of IEGs. Analysis of hippocampal areas revealed and supported this same hypothesis, as a significant increase of H4K5ac and p-Brd4 expression was seen but mRNA levels remained similar to control conditions.

4.3.1. *Influence of CPA on the transcript of Smarcc1*

SWI/SNF complex, in which Smarcc1 protein takes part, has shown to play a major role in transcriptional activity as a molecular switch controlling mRNA synthesis [69]. Nonetheless, its precise role into formation and recall of addictive memories is yet to be discovered. We found a significant lowering of *Smarcc1* mRNA levels after the retrieval of aversive memories both in the BLA and CA1. We could also see a slight decrease, although not significant, in the DG area during the same conditions. These results may seem conflicting, provided that p-Brd4 and H4K5ac levels may reflect an enhancement in transcription and therefore an increased need of Smarcc1 protein synthesis to form the complex. Not many studies have addressed the levels of *Smarcc1* as a potential effect of drugs of abuse and related memory formation and retrieval. To our knowledge, only one investigation has linked *Smarcc1* gene regulation with drug-related behaviour, resulting in upregulation after cocaine self-administration [57]. On the other hand, it has been shown a decrease in *Smarcc1* transcription in hippocampi of Down's syndrome mice foetuses [70]. In this line, and knowing that morphine-dependence processes are also related to cognitive impairments [71], our results might first suggest that *Smarcc1* mRNA regulation could be affected by drug-memory retrieval. Since mRNA is the substrate for protein synthesis, one plausible explanation may be that *Smarcc1* mRNA could have been synthesized right after the exposure to CPA-paired environment, but the stimulus was not strong enough to keep the *Smarcc1* synthesis running.

5. Conclusions

Chromatin remodelling and its effect on memory formation and retrieval caused by drugs of abuse have not been extensively studied. The present study shows that morphine-withdrawal aversive memories induced by CPA paradigm produced an increase of H4K5ac and p-Brd4 in BLA and hippocampus of morphine-dependent rats, which suggests that epigenetic activation may underlie aversive memory retrieval. After the extinction training, this increase was reverted, thus pointing out a more repressed state of the chromatin during this process. However, the epigenetic changes during CPA did not correlate with an increase of the transcription of IEGs, which may imply that other secondary targets might be already being subjected to the induction of transcription. Our results show that chromatin regulation could be an important mechanism involved in withdrawal-memory retrieval and the extinction of aversive memories. These findings may be helpful to uncover new molecular targets for new pharmacological approaches to address addictive disorders and avoid relapse, which is a major issue when treating addiction. However, further studies are needed to elucidate the complex mechanisms involved in memory formation and extinction induced by drugs of abuse and their effect on behaviour.

Funding information

This study was financially supported by MCIN/AEI/10.13039/501100011033 and by "ERDF A way of making Europe" (grants SAF2017–85679-R and PID2020–113557RB-I00), and by and by the Comunidad Autónoma de la Región de Murcia a través de la convocatoria de Ayudas a proyectos para el desarrollo de investigación científica y t é cnica por grupos competitivos, incluida en el Programa Regional de Fomento de la Investigación Científica y T é cnica de Excelencia (Plan de Actuación 2022) de la Fundación Séneca, Agencia de Ciencia y Tecnología de la Región de Murcia (grants 21133/SF/19; 21905/PI/22). Aurelio Franco-García is granted by "Ayuda para la Formación de Profesorado Universitario" program of MICINN (FPU19/01722). Victoria Gómez-Murcia is granted by "Programa Saavedra Fajardo" program of Fundación Séneca (21133/SF/19).

CRediT authorship contribution statement

Aurelio Franco-García (first author): Conceptualization, Investigation, Visualization, Data Curation and Writing—Original Draft. **Victoria Gómez-Murcia**: Investigation and Visualization. **Francisco José Fernández-Gómez**: Investigation. **Raúl González-Andreu**: Investigation. **Juana M. Hidalgo**: Investigation and Resources. **M. Victoria Milanés (co-corresponding author)**: Conceptualization, Validation, Formal analysis, Data Curation, Funding acquisition, Project administration, Supervision, and Writing—Original Draft. **Cristina Núñez (co-corresponding author):** Conceptualization, Validation, Formal analysis, Data Curation, Funding acquisition, Project administration, Supervision, review and editing. All authors have read and agreed to the published version of the manuscript.

Declaration of Competing Interest

The authors declare no competing financial interests.

Data availability

Data will be made available on request.

Appendix A. Supporting information

Supplementary data associated with this article can be found in the online version at doi:10.1016/j.biopha.2023.115055.

References

[1] R. Sinha, New findings on biological factors predicting addiction relapse vulnerability, Curr. Psychiatry Rep. 13 (2011) 398–405.
[2] C.P. O'Brien, Anticraving medications for relapse prevention: a possible new class of psychoactive medications, Am. J. Psychiatry 162 (8) (2005) 1423–1431.

[3] Y. Shaham, H. Rajabi, J. Stewart, Relapse to heroin-seeking in rats under opioid maintenance: the effects of stress, heroin priming, and withdrawal, J. Neurosci. 16 (5) (1996) 1957–1963.
[4] C.P. O'Brien, T. Testa, T.J. O'Brien, J.P. Brady, B. Wells, Conditioned narcotic withdrawal in humans, Science 195 (4282) (1977) 1000–1002.
[5] D. García-Pérez, S. Ferenczi, K.J. Kovács, M.L. Laorden, M.V. Milanés, C. Núñez, Glucocorticoid homeostasis in the dentate gyrus is essential for opiate withdrawal-associated memories, Mol. Neurobiol. 54 (8) (2017) 6523–6541.
[6] L. Stinus, S. Caille, G.F. Koob, Opiate withdrawal-induced place aversion lasts for up to 16 weeks, Psychopharmacol. (Berl.) 149 (2) (2000) 115–120.
[7] M. Cammarota, L.R. Bevilaqua, D.M. Barros, M.R. Vianna, L.A. Izquierdo, J. H. Medina, et al., Retrieval and the extinction of memory, Cell Mol. Neurobiol. 25 (3–4) (2005) 465–474.
[8] B.J. Everitt, Neural and psychological mechanisms underlying compulsive drug seeking habits and drug memories – indications for novel treatments of addiction, Eur. J. Neurosci. 40 (1) (2014) 2163–2182.
[9] D. García-Pérez, M.L. Laorden, M.V. Milanés, Acute Morphine, Chronic Morphine, and Morphine Withdrawal Differently Affect Pleiotrophin, Midkine, and Receptor Protein Tyrosine Phosphatase β/ζ Regulation in the Ventral Tegmental Area, Mol. Neurobiol. 54 (1) (2017) 495–510.
[10] Y.Y. Hou, B. Lu, M. Li, Y. Liu, J. Chen, Z.Q. Chi, et al., Involvement of actin rearrangements within the amygdala and the dorsal hippocampus in aversive memories of drug withdrawal in acute morphine-dependent rats, J. Neurosci. 29 (39) (2009) 12244–12254.
[11] D. García-Pérez, R. López-Bellido, R.E. Rodríguez, M.L. Laorden, C. Núñez, M. V. Milanés, Dysregulation of dopaminergic regulatory mechanisms in the mesolimbic pathway induced by morphine and morphine withdrawal, Brain Struct. Funct. 220 (4) (2015) 1901–1919.
[12] D. García-Pérez, C. Núñez, M.L. Laorden, M.V. Milanés, Regulation of dopaminergic markers expression in response to acute and chronic morphine and to morphine withdrawal, Addict. Biol. 21 (2) (2016) 374–386.
[13] D. Osorio-Gómez, M.I. Miranda, K. Guzmán-Ramos, F. Bermúdez-Rattoni, Transforming experiences: neurobiology of memory updating/editing, Front Syst. Neurosci. 17 (2023), 1103770.
[14] Y. Dong, J.R. Taylor, M.E. Wolf, Y. Shaham, Circuit and synaptic plasticity mechanisms of drug relapse, J. Neurosci. 37 (45) (2017) 10867–10876.
[15] J.R. Taylor, P. Olausson, J.J. Quinn, M.M. Torregrossa, Targeting extinction and reconsolidation mechanisms to combat the impact of drug cues on addiction, Neuropharmacology 56 (Suppl 1) (2009) 186–195.
[16] R. Guerrero-Bautista, B.R. Do Couto, J.M. Hidalgo, F.J. Cárceles-Moreno, G. Molina, M.L. Laorden, et al., Modulation of stress- and cocaine prime-induced reinstatement of conditioned place preference after memory extinction through dopamine D3 receptor, Prog. Neuropsychopharmacol. Biol. Psychiatry 92 (2019) 308–320.
[17] K.M. Myers, W.A. Carlezon, Extinction of drug- and withdrawal-paired cues in animal models: relevance to the treatment of addiction, Neurosci. Biobehav Rev. 35 (2) (2010) 285–302.
[18] C.J. Browne, A. Godino, M. Salery, E.J. Nestler, Epigenetic mechanisms of opioid addiction, Biol. Psychiatry 87 (1) (2020) 22–33.
[19] C.C.Y. Wong, J. Mill, C. Fernandes, Drugs and addiction: an introduction to epigenetics, Addiction 106 (2011) 480–489.
[20] D.M. Walker, H.M. Cates, E.A. Heller, E.J. Nestler, Regulation of chromatin states by drugs of abuse, Curr. Opin. Neurobiol. 30 (2015) 112–121.
[21] A.J. Robison, E.J. Nestler, Transcriptional and epigenetic mechanisms of addiction, Nat. Rev. Neurosci. 12 (11) (2011) 623–637.
[22] E.J. Nestler, C. Lüscher, The molecular basis of drug addiction: linking epigenetic to synaptic and circuit mechanisms, Neuron 102 (1) (2019) 48–59.
[23] C.C. Wong, J. Mill, C. Fernandes, Drugs and addiction: an introduction to epigenetics, Addiction 106 (3) (2011) 480–489.
[24] V.R. Rao, S.A. Pintchovski, J. Chin, C.L. Peebles, S. Mitra, S. Finkbeiner, AMPA receptors regulate transcription of the plasticity-related immediate-early gene Arc, Nat. Neurosci. 9 (7) (2006) 887–895.
[25] T. Kouzarides, Chromatin modifications and their function, Cell 128 (4) (2007) 693–705.
[26] Y. Han, A.A. Reyes, S. Malik, Y. He, Cryo-EM structure of SWI/SNF complex bound to a nucleosome, Nature 579 (7799) (2020) 452–455.
[27] F. Frenois, C. Le Moine, M. Cador, The motivational component of withdrawal in opiate addiction: role of associative learning and aversive memory in opiate addiction from a behavioral, anatomical and functional perspective, Rev. Neurosci. 16 (3) (2005) 255–276.
[28] M. Lucas, F. Frenois, C. Vouillac, L. Stinus, M. Cador, Le, C. Moine, Reactivity and plasticity in the amygdala nuclei during opiate withdrawal conditioning: differential expression of c-fos and arc immediate early genes, Neuroscience 154 (3) (2008) 1021–1033.
[29] B.J. Everitt, R.N. Cardinal, J.A. Parkinson, T.W. Robbins, Appetitive behavior: impact of amygdala-dependent mechanisms of emotional learning, Ann. N. Y Acad. Sci. 985 (2003) 233–250.
[30] B. Roozendaal, J.L. McGaugh, Memory modulation, Behav. Neurosc 125 (2011) 797–824.
[31] G. Schulteis, A. Markou, L.H. Gold, L. Stinus, G.F. Koob, Relative sensitivity to naloxone of multiple indices of opiate withdrawal: a quantitative dose-response analysis, J. Pharm. Exp. Ther. 271 (3) (1994) 1391–1398.
[32] D.M. Krolewski, A. Medina, I.A. Kerman, R. Bernard, S. Burke, R.C. Thompson, et al., Expression patterns of corticotropin-releasing factor, arginine vasopressin, histidine decarboxylase, melanin-concentrating hormone, and orexin genes in the human hypothalamus, J. Comp. Neurol. 518 (2010) 4591–4611.
[33] K.M. Myers, A.J. Bechtholt-Gompf, B.R. Coleman, W.A. Carlezon, Extinction of conditioned opiate withdrawal in rats in a two-chambered place conditioning apparatus, Nat. Protoc. 7 (3) (2012) 517–526.
[34] F. Frenois, M. Cador, S. Caille, L. Stinus, Le, C. Moine, Neural correlates of the motivational and somatic components of naloxone-precipitated morphine withdrawal, EurJNeurosci 16 (2002) 1377–1389.
[35] B. Pintér-Kübler, S. Ferenczi, C. Núnez, E. Zelei, A. Polyák, M.V. Milanés, et al., Differential Changes in Expression of Stress- and Metabolic-Related Neuropeptides in the Rat Hypothalamus during Morphine Dependence and Withdrawal, PLoS One 8 (6) (2013), e67027.
[36] S. Ferenczi, C. Núñez, B. Pintér-Kübler, A. Földes, F. Martín, V.L. Márkus, et al., Changes in metabolic-related variables during chronic morphine treatment, Neurochem Int 57 (3) (2010) 323–330.
[37] S. Ferenczi, C. Núñez, B. Pinter-Kebler, A. Foldes, F. Martín, M.V. Milanés, et al., Changes in metabolic-related variables during chronic morphine treatment, NeurochemInt 53 (2010) 323–330.
[38] G. Paxinos, C. Watson. The rat brain in stereotaxic coordinates, 6th ed..,, Academic Press,, Amsterdam, 2007 2007.
[39] K.W. Dunn, M.M. Kamocka, J.H. MacDonald, A practical guide to evaluating colocalization in biological microscopy, Am. J. Physiol. Cell Physiol. 300 (2011) C723–C742.
[40] S.V. Costes, D. Daelemans, E.H. Cho, Z. Dobbin, G. Pavlakis, S. Lockett, Automatic and quantitative measurement of protein-protein colocalization in live cells, Biophys. J. 86 (6) (2004) 3993–4003.
[41] M. Benavides, M.L. Laorden, J.C. García-Borrón, M.V. Milanés, Regulation of tyrosine hydroxilase levels and activity and Fos expression during opioid withdrawal in the hypothalamic PVN and medulla oblongata catecholaminergic cell groups innervating the PVN, Eur. J. Neurosci. 17 (2003) 103–112.
[42] J. Navarro-Zaragoza, C. Núñez, J. Ruiz-Medina, M.L. Laorden, O. Valverde, M. V. Milanés, CRF(2) mediates the increased noradrenergic activity in the hypothalamic paraventricular nucleus and the negative state of morphine withdrawal in rats, Br. J. Pharm. 162 (2012) 851–862.
[43] W. Zhang, C. Prakash, C. Sum, Y. Gong, Y. Li, J.J. Kwok, et al., Bromodomain-containing protein 4 (BRD4) regulates RNA polymerase II serine 2 phosphorylation in human CD4+ T cells, J. Biol. Chem. 287 (51) (2012) 43137–43155.
[44] X. Hu, X. Lu, R. Liu, N. Ai, Z. Cao, Y. Li, et al., Histone cross-talk connects protein phosphatase 1α (PP1α) and histone deacetylase (HDAC) pathways to regulate the functional transition of bromodomain-containing 4 (BRD4) for inducible gene expression, J. Biol. Chem. 289 (33) (2014) 23154–23167.
[45] T. Takizawa, E. Meshorer, Chromatin and nuclear architecture in the nervous system, Trends Neurosci. 31 (7) (2008) 343–352.
[46] J.-F. Liu, J. Tian, J.-X. Li, Modulating reconsolidation and extinction to regulate drug reward memory, Eur. J. Neurosci. 50 (3) (2019) 2503–2512.
[47] P.D. Rivera, S.J. Simmons, R.P. Reynolds, A.L. Just, S.G. Birnbaum, A.J. Eisch, Image-guided cranial irradiation-induced ablation of dentate gyrus neurogenesis impairs extinction of recent morphine reward memories, Hippocampus 29 (8) (2019) 726–735.
[48] B. Huang, Y. Li, D. Cheng, G. He, X. Liu, L. Ma, β-Arrestin-biased β-adrenergic signaling promotes extinction learning of cocaine reward memory, Sci. Signal 11 (512) (2018).
[49] D. García-Pérez, S. Ferenczi, K.J. Kovács, M.V. Milanés, Distinct regulation pattern of Egr-1, BDNF and Arc during morphine-withdrawal conditioned place aversion paradigm: Role of glucocorticoids, Behav. Brain Res 360 (2019) 244–254.
[50] C.S. Park, H. Rehrauer, I.M. Mansuy, Genome-wide analysis of H4K5 acetylation associated with fear memory in mice, BMC Genom. 14 (2013) 539.
[51] J. Gräff, L.H. Tsai, Histone acetylation: molecular mnemonics on the chromatin, Nat. Rev. Neurosci. 14 (2) (2013) 97–111.
[52] W. Renthal, E.J. Nestler, Histone acetylation in drug addiction, Semin Cell Dev. Biol. 20 (4) (2009) 387–394.
[53] A. Kumar, K.H. Choi, W. Renthal, N.M. Tsankova, D.E. Theobald, H.T. Truong, et al., Chromatin remodeling is a key mechanism underlying cocaine-induced plasticity in striatum, Neuron 48 (2) (2005) 303–314.
[54] J. Sheng, Z. Lv, L. Wang, Y. Zhou, B. Hui, Histone H3 phosphoacetylation is critical for heroin-induced place preference, Neuroreport 22 (12) (2011) 575–580.
[55] G. Egervari, J. Landry, J. Callens, J.F. Fullard, P. Roussos, E. Keller, et al., Striatal H3K27 Acetylation Linked to Glutamatergic Gene Dysregulation in Human Heroin Abusers Holds Promise as Therapeutic Target, Biol. Psychiatry 81 (7) (2017) 585–594.
[56] G.C. Sartor, S.K. Powell, S.P. Brothers, C. Wahlestedt, Epigenetic Readers of Lysine Acetylation Regulate Cocaine-Induced Plasticity, J. Neurosci. 35 (45) (2015) 15062–15072.
[57] A. Sadakierska-Chudy, M. Frankowska, J. Jastrzębska, K. Wydra, J. Miszkiel, M. Sanak, et al., Cocaine Administration and Its Withdrawal Enhance the Expression of Genes Encoding Histone-Modifying Enzymes and Histone Acetylation in the Rat Prefrontal Cortex, Neurotox. Res 32 (1) (2017) 141–150.
[58] M. Malvaez, E. Mhillaj, D.P. Matheos, M. Palmery, M.A. Wood, CBP in the nucleus accumbens regulates cocaine-induced histone acetylation and is critical for cocaine-associated behaviors, J. Neurosci. 31 (47) (2011) 16941–16948.
[59] W. Renthal, I. Maze, V. Krishnan, H.E. Covington, G. Xiao, A. Kumar, et al., Histone deacetylase 5 epigenetically controls behavioral adaptations to chronic emotional stimuli, Neuron 56 (3) (2007) 517–529.
[60] Y.X. Xue, Y.X. Luo, P. Wu, H.S. Shi, L.F. Xue, C. Chen, et al., A memory retrieval-extinction procedure to prevent drug craving and relapse, Science 336 (6078) (2012) 241–245.
[61] J.T. Lloyd, K.C. Glass, Biological function and histone recognition of family IV bromodomain-containing proteins, J. Cell Physiol. 233 (3) (2018) 1877–1886.

[62] W.S. Wang, S. Kang, W.T. Liu, M. Li, Y. Liu, C. Yu, et al., Extinction of aversive memories associated with morphine withdrawal requires ERK-mediated epigenetic regulation of brain-derived neurotrophic factor transcription in the rat ventromedial prefrontal cortex, J. Neurosci. 32 (40) (2012) 13763–13775.
[63] A. Franco-García, F.J. Fernández-Gómez, V. Gómez-Murcia, J.M. Hidalgo, M. V. Milanés, C. Núñez, Molecular Mechanisms Underlying the Retrieval and Extinction of Morphine Withdrawal-Associated Memories in the Basolateral Amygdala and Dentate Gyrus, Biomedicines 10 (3) (2022).
[64] O. Gilan, I. Rioja, K. Knezevic, M.J. Bell, M.M. Yeung, N.R. Harker, et al., Selective targeting of BD1 and BD2 of the BET proteins in cancer and immunoinflammation, Science 368 (6489) (2020) 387–394.
[65] J. Jones-Tabah, R.D. Martin, J.J. Chen, J.C. Tanny, P.B.S. Clarke, T.E. Hébert, A role for BET proteins in regulating basal, dopamine-induced and cAMP/PKA-dependent transcription in rat striatal neurons, Cell Signal 91 (2022), 110226.
[66] J.M. Sullivan, A. Badimon, U. Schaefer, P. Ayata, J. Gray, C.W. Chung, et al., Autism-like syndrome is induced by pharmacological suppression of BET proteins in young mice, J. Exp. Med 212 (11) (2015) 1771–1781.
[67] V. Ramirez-Amaya, A. Angulo-Perkins, M.K. Chawla, C.A. Barnes, S. Rosi, Sustained transcription of the immediate early gene Arc in the dentate gyrus after spatial exploration, J. Neurosci. 33 (4) (2013) 1631–1639.
[68] N. Ai, X. Hu, F. Ding, B. Yu, H. Wang, X. Lu, et al., Signal-induced Brd4 release from chromatin is essential for its role transition from chromatin targeting to transcriptional regulation, Nucleic Acids Res 39 (22) (2011) 9592–9604.
[69] L. Yan, S. Xie, Y. Du, C. Qian, Structural Insights into BAF47 and BAF155 Complex Formation, J. Mol. Biol. 429 (11) (2017) 1650–1660.
[70] W.L. Shi, Z.Z. Liu, H.D. Wang, D. Wu, H. Zhang, H. Xiao, et al., Integrated miRNA and mRNA expression profiling in fetal hippocampus with Down syndrome, J. Biomed. Sci. 23 (1) (2016) 48.
[71] R.K. McNamara, R.W. Skelton, Pharmacological dissociation between the spatial learning deficits produced by morphine and diazepam, Psychopharmacol. (Berl.) 108 (1–2) (1992) 147–152.